THE JOURNAL OF PHYSICAL CHEMISTRY B

ARTICLE

pubs.acs.org/JPCB

Enhancement in Adsorption and Catalytic Activity of Enzymes Immobilized on Phosphorus- and Calcium-Modified MCM-41

Kuwahara Yasutaka, Yamanishi Takato, Kamegawa Takashi, Mori Kohsuke, and Yamashita Hiromi*

Division of Materials and Manufacturing Science, Graduate School of Engineering, Osaka University, 2-1 Yamadaoka, Suita, Osaka 565-0871, Japan

Supporting Information

ABSTRACT: An oxidative enzyme, horseradish peroxidase (HRP), was immobilized on phosphorus- and/or calcium-modified MCM-41 mesoporous silicas with suitable pore diameters. Structural analyses by means of XRD and nitrogen adsorption confirmed that the P- and/or Ca-modified MCM-41 materials retained their structural quality even after the modification or the enzyme immobilization. Detailed studies of the adsorption behaviors and characterization using FT-IR spectroscopy and zeta potential measurements revealed that the P and Ca atoms attached on the silica surface provided increased uptake of HRP molecules, which is attributable to the more negatively charged surface or strong interatomic interactions between these atoms and the functional groups of the enzyme. In particular, P-modified MCM-41 showed an improved adsorption capacity in a short adsorption period and over a wide pH range without denaturation of the protein structure, in which the largest HRP adsorption capacity was 154 mg/g. Furthermore, HRP immobilized on P-modified MCM-41 showed higher enzymatic activity and reusability in the oxidation of 1,2-diaminobenzene in an organic solvent at a temperature of 37 °C than that immobilized on the parent MCM-41. This enhancement in enzymatic activity can be related to the structural integrity of loaded HRP molecules and the strong adsorption on the P-MCM-41 surface. This work thus demonstrates that mesoporous silica bearing P and/or Ca atoms can provide a surface environment suitable for enzyme immobilization.

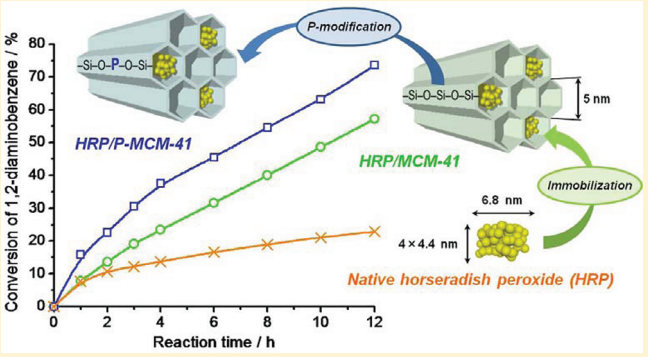

INTRODUCTION

In recent years, adsorption and immobilization of biological molecules such as proteins and enzymes on inorganic materials have been attractive for a range of applications in biotechnology including food processing, enzymatic catalysis, drug-delivery systems, and biosensors.[1−4] In particular, enzymes have a high substrate specificity and reactive efficiency under ambient conditions as biocatalysts compared to artificial inorganic catalysts. Nevertheless, the harsh conditions required for chemical reactions limit their applicability because it is difficult to maintain their highly complex molecular configurations. Such emerging scientific and technological demands have necessitated the use of periodic nanoporous silicates, whose diameters are approximately comparable to the diameters of the biomolecules.[5−8] Generally, mesoporous silica (MPS) materials have ordered arrays of pores with tunable pore diameters (2−20 nm), large surface areas, and diverse pore geometries. With pore sizes suitable for the uptake of larger molecules and with unique structural features, MPS has been envisaged as a promising carrier material for biomolecules with which stable storage would be achieved and the separation and reuse of biomolecules would be simplified.[9−14] A wide range of investigations concerning the adsorption and immobilization of biomolecules on various types of MPS materials have been reported so far. For example, Takahashi et al. carried out the encapsulation of horseradish peroxidase (HRP) in some types of MPS materials with different pore diameters and reported that the FSM-16 and MCM-41 families with hexagonal porous arrays and suitable pore diameters highly stabilize enzymes.[15]

Current research on this issue has mainly aimed at the functionalization of the silica surface, that is, the modification of organic groups by direct/postsynthetic methods using a variety of organosilanes. It has been found that MPS materials bearing different surface functional groups (e.g., −SH, $-(CH_2)_n$, −Ph, −Cl, $-NH_2$, and −COOH) efficiently immobilize specific enzymes through either electrostatic or hydrophilic−hydrophobic mechanisms.[9,16−19] Further, immobilization through covalent bonds ensures strong binding and negligible leaching, for which an aldehyde-functionalized MPS has been commonly used.[20] However, these organic modification routes require complicated procedures, toxic organic solvents, and high costs in support preparation. Physical adsorption is, indeed, the simplest method

Received: April 19, 2011
Revised: July 21, 2011
Published: July 21, 2011

for immobilizing enzymes onto MPS materials without affecting the active sites and disruption of subunits; however, leaching of enzymes into the reaction medium is a major problem because of weak interactions between enzymes and the MPS surface.

Another advantageous characteristic of MPS is the introduction of foreign altervalent ions (e.g., Al, Ga, Sn, Ti, V, and Zr) into the silica matrix by direct/postsynthetic procedures, through which multifunctionality (e.g., acid−base and/or redox sites) can be added to the MPS and, thus, highly elaborated nanomaterials and catalytic systems can be designed.[21−23] Concerning biomolecule−MPS conjugated systems, tremendous attention has mostly been paid to the effects of structural factors, such as pore diameter, pore volume, geometry, and dimensions, on the adsorption capacity;[12−15] however, little attention has been paid to the effects of heteroatoms on the adsorption or catalytic activity of enzymes.[24] The modification of a silica surface with specific elements might dramatically change the adsorption and enzymatic properties of biomolecules.

In this study, we propose a methodology to improve the adsorption properties of MPS materials for biomolecules. This was achieved by embedding biocompatible elements, namely, phosphorus and/or calcium, in the MPS silica matrix. A silicate material including Ca and P, as well as Mg and Na, ions, namely, bioactive glass, exhibits biocompatibility and has been utilized as a biomimic material in bioimplanting.[25−28] Furthermore, such bioactive glasses and the related calcium phosphate compounds, exemplified by hydroxyapatite, have been well-known to have excellent adsorption properties for proteins.[29,30] These atoms with a biocompatible character could potentially contribute to the adsorption property for biomolecules. The focus of this article is the preparation and characterization of P- and Ca-modified MPS materials, as well as the investigation of the effects of the P and Ca atoms on the structures, adsorption behaviors, and enzymatic activities of biomolecules. It is required for an adsorbent to have a large pore diameter and a large pore volume, which is essential to accommodate a large quantity of biomolecules in the mesoporous channels. In this study, MCM-41 with a hexagonal array of one-dimensional channels was employed as a support material, and its pore size was extended by the addition of the swelling agents mesitylene (MES) and 1,3,5-triisopropylbenzene (TIPB) according to the literature method.[31] Among the various types of enzymes, HRP, an oxidative enzyme with molecular dimensions of 4.0 × 4.4 × 6.8 nm and a molecular weight of approximately 44000, was chosen.[7] The textural properties of the MCM-41 adsorbents before and after HRP immobilization were investigated by X-ray diffraction (XRD) and N_2 sorption measurements. The effects of the P and Ca atoms on the structures, adsorption behaviors, and enzymatic activities of HRP were studied in detail. The residual enzymatic activities of HRP were evaluated by the oxidation reaction of 1,2-diaminobenzene in an organic solvent.

EXPERIMENTAL SECTION

Materials. Horseradish peroxidase [HRP, EC.1.11.1.7, activity 250 U/mg of protein (diagnostic reagent grade)] was purchased from Toyobo Enzymes Inc. Ovalbumin (OVA) was obtained from Nacalai Tesque Inc. Water glass (SiO_2/Na_2O = 2.18) and silica powder (Cab-o-sil M-5) as silicon sources for mesoporous silica were purchased from Wako Pure Chemical Industries, Ltd., and Aldrich, respectively. Surfactants, swelling agents, triethoxyphosphate (TEP), and calcium nitrate [$Ca(NO_3)_2$] were purchased from Tokyo Chemical Industry Co., Ltd. Solvents and all commercially available organic compounds for chemical reactions were purified using standard procedures.

Preparation of Phosphorus- and/or Calcium-Modified MCM-41. A large-pore MCM-41 material with an average pore diameter of 4.9 nm was prepared from water glass by using dodecyltrimethylammonium bromide (C_{12}TAB) and hexadecyltrimethylammonium bromide (C_{16}TAB) as surfactants and mesitylene (MES) and 1,3,5-triisopropylbenzene (TIPB) as swelling agents with molar ratios of MES/surfactant = 1.0 and TIPB/surfactant = 1.0, according to the method reported by Lindlar et al.[31] In a typical synthesis, water glass (14.76 g) and Cab-o-sil (4.15 g) were dissolved in distilled water (60 mL). The mixture was stirred at room temperature for 1 h until a homogeneous clear solution obtained. Then, an aqueous solution containing C_{12}TAB (1.00 g), C_{16}TAB (7.00 g), MES (2.78 g), and TIPB (4.85 g) was added dropwise to this solution, which was stirred vigorously at room temperature for 3 h. The chemical composition of the initial gel was adjusted to be $Na_2O/SiO_2/C_{12}TAB/C_{16}TAB/MES/TIPB/H_2O$ = 0.26:1:0.02:0.12:0.14:0.14:40. The pH of the above solution was adjusted to 11.0 by adding a portion of dilute acetic acid solution. Subsequently, the mixture was transferred into a stainless steel autoclave and kept in an oven at 105 °C for 4 h under static conditions. The resultant product was filtered, washed with a sufficient amount of deionized water, and dried at 100 °C overnight, after which it was subjected to calcination at 550 °C in air to remove the surfactants.

Phosphorus- and/or calcium-modified MCM-41 materials were prepared by an impregnation method using TEP and $Ca(NO_3)_2$ as the P and Ca sources, respectively.[32−34] Typically, MCM-41 powder (0.5 g) was suspended in an aqueous solution (50 mL) containing an adequate amount of TEP and/or $Ca(NO_3)_2$, and the mixture was stirred for 12 h at room temperature. For modification with TEP, the pH of the mixed solution was adjusted to below 2.0 by adding dilute HCl solution to facilitate the hydrolysis and condensation. The resultant suspension was evaporated under a vacuum, dried at 100 °C overnight, and finally calcined at 550 °C in air. The samples are denoted as Ca_xP_y-MCM-41, where x and y indicate the Ca/Si and P/Si molar ratios (expressed as percentages), respectively, in the initial solution.

Characterization. The X-ray powder diffraction (XRD) patterns of mesoporous silica materials before and after the enzyme immobilization were recorded on a Rigaku Ultima IV diffractometer with Cu Kα radiation (λ = 1.54056 Å). Scans were performed at a step size of 0.02° (2θ) over the 2θ range 0.6−60°. Elemental analysis was performed using-energy dispersive X-ray fluorescence spectrometry (EDX; EDAX Ltd., DX-4). Field-emission transmission electron microscopy (FE-TEM) images were obtained with a Hitachi Hf-2000 FE-TEM instrument equipped with a Kevex energy-dispersive X-ray detector operated at 200 kV. N_2 adsorption−desorption isotherms were measured at −196 °C using a BELSORP-max system (BEL JAPAN, Inc.). All samples before enzyme adsorption were degassed at 350 °C for 3 h prior to the measurements, whereas enzyme-loaded samples were degassed at 40 °C for 12 h. Specific surface areas were calculated by the BET (Brunauer−Emmett−Teller) method using adsorption data in the relative pressure range of P/P_0 = 0.05−0.35. Pore size distributions were obtained from the adsorption branch of the N_2 isotherms by the BJH (Barrett−Joyner−Halenda) method. FT-IR spectra of mesoporous silica materials before and after enzyme immobilization were recorded

on a JASCO FT/IR-6100 instrument in the spectral range of 2000−400 cm^{-1} under a vacuum with a resolution of 4 cm^{-1}. Zeta potentials were measured with an ELSZ-1 apparatus (Otsuka Electronics Co. Ltd.) at 25 °C, for samples diluted with deionized water (1 mg/mL). Each sample was measured three times, and the average value was used.

Protein Adsorption and Enzyme Immobilization. The adsorption of OVA was performed according to the following procedure: MCM-41 powder (100 mg) was suspended in 2 mL of 50 mM sodium phosphate buffer solution (pH 7.0) containing OVA (10 mg/mL) in a centrifuge tube. The mixture was continuously stirred at 15 °C for 12 h and then centrifuged at 20000*g* for 10 min, the resulting product being filtered out, washed with 50 mL of deionized water, and then desiccated in vacuo at room temperature. The immobilization of HRP enzyme on the mesoporous silica materials was performed in the same manner but under stirring at 4 °C to prevent denaturation. The time dependence of the amount of enzyme adsorbed was examined by varying the adsorption time. For the pH profile of enzyme adsorption, HRP was adsorbed onto MCM-41 powder in 50 mM sodium acetate buffer (for pH 3.0 and 5.0), 50 mM sodium phosphate buffer (for pH 7.0), or 50 mM glycine (Gly)−NaOH buffer (for pH 9.0 and 11.0). The amounts of proteins adsorbed on the mesoporous silica solids were determined from the weight losses at temperatures from 100 to 1000 °C under an air flow by thermal gravimetric analysis, which was carried out with a differential thermal analysis−thermogravimetry (DTA−TG) instrument (MAC Science Co. Ltd., TG-DTA2000S) at a heating rate of 10 °C/min using α-Al_2O_3 as the standard. The supported HRP was stored at 4 °C in the refrigerator until use.

Measurement of Enzymatic Activity in an Organic Solvent. To evaluate the enzymatic activity of HRP immobilized on mesoporous silica (at pH 7.0 for 12 h), the oxidative reaction of 1,2-diaminobenzene in toluene using *tert*-butyl hydroperoxide (TBHP) as the organic oxidant was selected. A portion (10 mL) of 100 mM 1,2-diaminobenzene in anhydrous toluene and 2.5 mL of 1.1 M TBHP in decane were mixed in a round-bottom flask. The reaction was initiated by adding supported HRP containing 1.0 mg of enzyme or 1.0 mg of the native enzyme with constant stirring at 37 °C. The conversion of 1,2-diaminobenzene was spectroscopically monitored by measuring the absorbance of the supernatant at 420 nm using a Shimadzu UV-2450 photospectrometer.[35] The corresponding weights of mesoporous silica solids without enzymes were also used to measure the background value (X_{bg}). The reusability of enzyme was also studied at least three times for a given supported HRP sample. After each reaction, the product mixture was centrifuged, and the separated solid catalyst was subjected to further reaction after being washed with 10 mL of toluene. The residual enzymatic activity (A_{res}) was determined with the equation

$$A_{res}\ (\%) = (X_x - X_{bg})/(X_1 - X_{bg}) \times 100$$

where X_x represents the conversion of 1,2-diaminobenzene occurring in 12 h of the *x*th reaction run (x = 1−4).

RESULTS AND DISCUSSION

Structural Analyses of MCM-41 Materials. The quality and structural change of the synthesized MCM-41 materials were assessed by powder XRD measurements. Figure 1A shows the XRD diffraction patterns of the pore-expanded MCM-41 materials. All samples exhibited an intense diffraction peak assignable to the (100) plane at 2θ = 1.31−1.36° and two broad peaks assignable to (110) and (210) in the low-angle region, although the (200) reflection is not distinguishable because of overlap with the (110) signal, reflecting a low regularity in the hexagonal pore arrangement. Addition of swelling agents, namely, MES and TIPB, caused a shift of the (100) reflection to lower 2θ value, as well as an increase in *d* spacings and unit-cell constants. The unit-cell constant a_0 of pore-expanded MCM-41 calculated from the (100) reflection was 7.77 nm, whereas that of the original MCM-41 synthesized without swelling agents was 4.32 nm, clearly indicating that the MCM-41 material synthesized with swelling agents had a larger pore diameter. The peak intensities of the (100) reflection and the unit-cell parameters were scarcely changed even after P and/or Ca modification; however, the peak intensities of the (110) and (210) reflections clearly decreased, indicating a partial loss of the long-range ordering of the porous structure upon the modification. In the high-angle region (Figure 1A), any peaks assignable to crystalline phases such as phosphorus oxide, calcium oxide, and calcium phosphate species was not distinguishable, except for a broad peak at around 15−35° that can be assigned to the amorphous silicate phase of the MCM-41 wall, implying that the P and Ca atoms are uniformly incorporated onto the silica surface of MCM-41. The results of chemical analysis confirmed the presence of expected amounts of P and Ca atoms within the samples (Table 1); however, the incorporated amounts of P atoms in P_{20}-MCM-41 and P_{40}-MCM-41 were smaller than the added amounts because of the low condensation polymerization rate between TEP and the hydrated silica surface.[36]

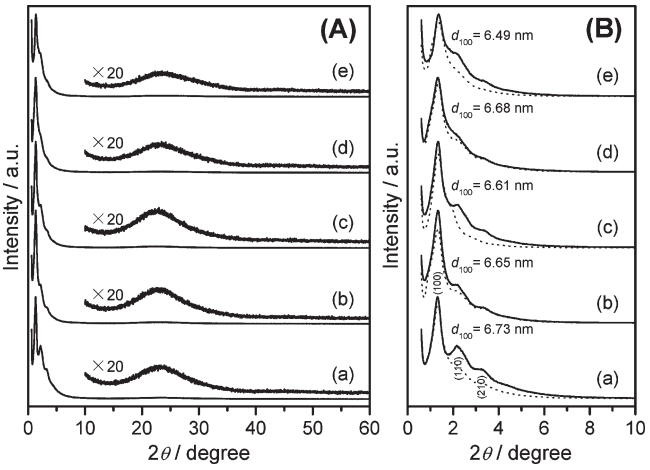

Figure 1. Powder XRD patterns (A) of as-prepared MCM-41 materials and (B) in the low-angle region before (solid lines) and after (dotted lines) HRP immobilization: (a) MCM-41, (b) P_{10}-MCM-41, (c) P_{40}-MCM-41, (d) Ca_5P_5-MCM-41, and (e) Ca_{10}-MCM-41.

Structural ordering of the prepared MCM-41 materials was further confirmed by TEM (Figure 1S, Supporting Information). The side-view TEM image of the parent MCM-41 (Figure 1SA, Supporting Information) clearly showed linearly aligned one-dimensional pore channels arranged at regular intervals, with an average pore size estimated to be ca. 4.9 nm. However, any ordered hexagonal structure was scarcely observed in the TEM image (Figure 1SB, Supporting Information), suggesting a disordered arrangement of the pores. This is related to the broader distribution of pore sizes compared to that in conventional MCM-41,

Table 1. Textural Properties of MCM-41 Materials and Adsorbed Amounts of OVA and HRP

	final molar ratio[a]		XRD		N_2 adsorption−desorption				adsorbed amounts	
adsorbent	Ca/Si	P/Si	d spacing (nm)	a_0[b] (nm)	S_{BET}[c,d] (m^2/g)	d_p[d,e] (nm)	V_p[d] (cm^3/g)	Occupancy[f] (%)	OVA[g] (mg/g)	HRP[h] (mg/g)
MCM-41	–	–	6.73	7.77	946 (609)	4.9 (4.8)	1.38 (0.85)	38	119	125
Ca_{10}-MCM-41	0.101	–	6.49	7.50	774 (412)	4.7 (4.6)	1.06 (0.59)	44	137	127
Ca_5P_5-MCM-41	0.068	0.061	6.68	7.71	835 (449)	4.8 (4.5)	1.11 (0.62)	44	152	128
P_{10}-MCM-41	–	0.093	6.65	7.68	864 (580)	4.9 (4.8)	1.14 (0.67)	41	133	140
P_{20}-MCM-41	–	0.149	6.64	7.67	848 (397)	4.7 (4.5)	1.11 (0.59)	47	134	146
P_{40}-MCM-41	–	0.192	6.61	7.63	786 (258)	4.6 (4.4)	1.02 (0.41)	60	136	154

[a] Determined from EDX analysis. [b] Unit cell constant calculated as $a_0 = d_{100} \times 2/\sqrt{3}$. [c] Calculated from the adsorption branch of the N_2 isotherm by the BET (Brunauer−Emmett−Teller) method. [d] Values in parentheses are those obtained after HRP immobilization at pH 7, buffer concentration = 50 mM, T = 4 °C, adsorption time = 12 h. [e] Calculated by the BJH (Barrett−Joyner−Halenda) method. [f] Spatial occupancy rate calculated as [1 − (pore volume remaining after HRP immobilization)/(total pore volume)] × 100. [g] Ovalbumin. [h] Horseradish peroxidase.

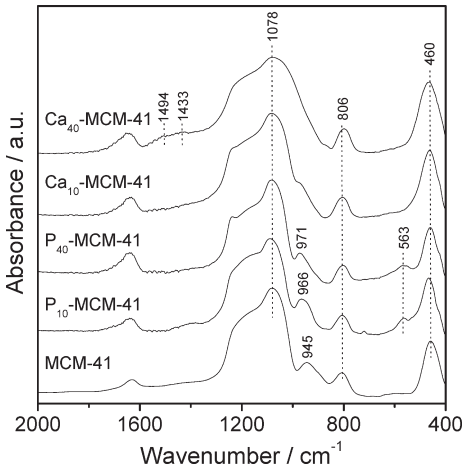

Figure 2. Infrared spectra of MCM-41, P-modified MCM-41, and Ca-modified MCM-41 materials.

which hinders the arrangement into perfect hexagonal arrays of pores. Significantly, the TEM images revealed that the porous structure and the expanded pore size were maintained even after P and/or Ca modification (Figure 1SC−F, Supporting Information).

Figure 2 shows FT-IR spectra of MCM-41 and P- or Ca-modified MCM-41 materials with different modification levels. The parent MCM-41 material exhibited some expected absorption bands at 460, 806, and 1078 cm^{-1} that are assignable to Si−O−Si stretching vibration and at 945 cm^{-1} that is assignable to Si−OH bond stretching. P-modified MCM-41 showed an additional absorption band at around 563 cm^{-1} that corresponds to $\nu_4(PO_4^{3-})$, although other absorption bands ascribable to the PO_4^{3-} tetrahedral unit were hard to identify because of the overlapping of the absorption bands of the silica matrix. Generally, this $\nu_4(PO_4^{3-})$ mode exhibits several absorption bands in the range of 520−660 cm^{-1}, and the splitting of this vibrational band reflects the degree of site symmetry of PO_4^{3-} groups.[37] A distinguishable intense peak observed in the infrared spectra of the P-MCM-41 materials indicates the presence of symmetric PO_4^{3-} species. Furthermore, a peak assigned to Si−OH bond stretching (945 cm^{-1}) shifted to higher frequencies upon P modification and eventually located at 971 cm^{-1}, which is identical to the position of $\nu_1(PO_4^{3-})$, suggesting the formation of Si−O−P linkages through dehydroxylation between surface silanol groups and TEP. These observations indicate that the P atoms were present on the silica surface presumably forming isolated $(O{=})P(—OH)_x(—O—Si{\equiv})_y$ ($x + y = 3$) moieties. On the other hand, in the FT-IR spectra of the Ca-modified MCM-41 materials, a decrease in the intensity of the band corresponding to Si−OH bond stretching was observed upon Ca modification, accompanied by the broadening of the Si−O−Si absorption band. Such a change in infrared spectra can be explained by the formation of Si−O−Ca−O−Si linkages so as to compensate the positive charge of Ca^{2+}. Additionally, two broad absorption bands assignable to carbonate species (CO_3^{2-}) physisorbed from the air were also observed at around 1433 and 1494 cm^{-1} as the Ca content was increased to Ca/Si > 0.4. This is due to the strong basicity of Ca atoms on the MCM-41 surface.[33,34] These FT-IR observations suggested the local formation of phosphosilicate and calciumsilicate on the MCM-41 surface.

In the N_2 adsorption measurements, all of the samples displayed type IV isotherms with capillary condensation and an H2-type hysteresis loop (Figure 3, circle), reflecting the presence of mesopore channels with broad pore distributions. Capillary condensation occurred at much higher relative pressure (P/P_0 = 0.6) than for MCM-41 synthesized without swelling agents ($P/P_0 \approx 0.3$), indicating that the pore diameter of MCM-41 increased substantially upon the addition of MES and TIPB. Based on the N_2 adsorption isotherms, it was found that pore diameter increased from 2.60 to 4.90 nm upon pore enlargement, in good agreement with the results of XRD and TEM measurements. The HRP molecule is elongated, and the narrowest cross section of the HRP molecule is ca. 4.0 nm × 4.4 nm.[7] These geometric dimensions also suggest that an MCM-41 material with a pore diameter of 4.9 nm is able to accommodate HRP molecules in its mesoporous channels. Furthermore, the specific pore volume increased from 0.86 to 1.38 cm^3/g, which is sufficient to accommodate a large quantity of biomolecules.

The textural parameters obtained from N_2 adsorption isotherms are reported in Table 1. A decrease in specific surface area and pore volume was observed after P and/or Ca modification, whereas the average pore diameter scarcely changed. In particular, Ca modification caused more significant damage to the mesoporous structure than modification with P atoms. As the added amounts of modifier agents increased, these parameters decreased more markedly, yet pore volume sufficient for accommodating enzymes remained. Such structural damage appeared to be dependent on the kind and amount of modifiers. An independent synthetic experiment using diammonium hydrogenphosphate [$(NH_4)_2HPO_4$]

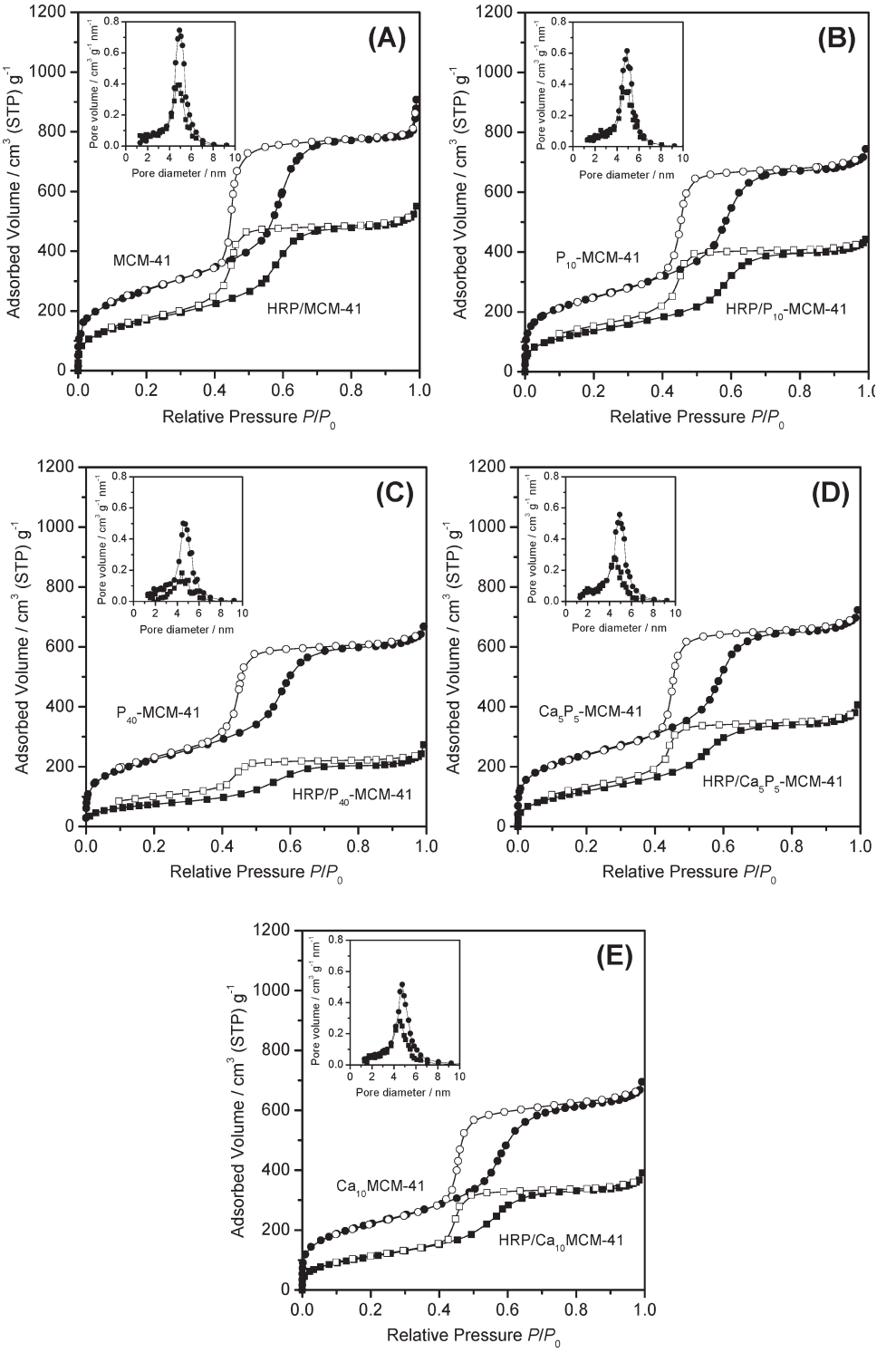

Figure 3. Nitrogen adsorption−desorption isotherms of (A) MCM-41, (B) P_{10}-MCM-41, (C) P_{40}-MCM-41, (D) Ca_5P_5-MCM-41, and (E) Ca_{10}-MCM-41 before and after HRP immobilization. Solid and open symbols represent adsorption and desorption isotherms, respectively. The insets show BJH pore size distributions.

as a phosphorus source resulted in lower pore regularity than the use of TEP. To preserve the original geometry of MCM-41, alkoxide precursors seem to be suited for this use. In addition, the use of excess amounts of $Ca(NO_3)_2$ (Ca/Si > 0.2) led to a crucial loss of mesoporous structure. Modification with Ca is likely to cause a detrimental effect on the silica network, probably because of its basic nature, that can lead to the cleavage of siloxane bonding and to the formation of amorphous calciumsilicate species during the modification process, as also suggested by FT-IR measurements.[33,34]

Adsorption of Enzyme on Mesoporous Silicas. To clarify whether HRP molecules are immobilized inside the mesoporous

channels or on the external surface, the MCM-41 materials after immobilization of HRP (adsorbed at pH 7, buffer concentration = 50 mM, T = 4 °C, adsorption time = 12 h) were also evaluated by powder XRD and N_2 adsorption measurements. From the adsorption studies, we found that most of the enzyme could be adsorbed within 12 h, so that an adsorption time of 12 h was employed as a standard in this work.

As shown in Figure 1B, the XRD patterns of the HRP-immobilized samples also exhibited strong diffraction peaks assigned to the (100) plane with intensities similar to those of the as-prepared samples, confirming sufficient structural stability of MCM-41 as a carrier for enzymes. However, the peak intensities of the (110) and (210) reflections clearly decreased after the HRP immobilization. Similar observations were made for enzyme immobilization on MCM-41, SBA-15, and KIT-6 by Vinu et al.[14,24] This reduced peak intensity is associated with occlusion of the mesopore channels by HRP molecules.

The degree of HRP immobilization in the mesochannels of the MCM-41 materials was quantified by N_2 adsorption measurements. The N_2 adsorption−desorption isotherms and pore size distribution curves of the MCM-41 materials before and after HRP immobilization are shown in Figure 3, and the textural parameters obtained from N_2 adsorption isotherms are summarized in Table 1. In all MCM-41 materials investigated here, the adsorbed amounts of nitrogen were markedly reduced, and the peaks of the pore size distribution curves decreased in height after HRP immobilization (Figure 3). As can be seen in Table 1, after HRP immobilization, the specific surface area and pore volume of MCM-41 decreased from 946 to 609 m^2/g and from 1.38 to 0.85 cm^3/g, respectively, which corresponds to a spatial occupancy rate of 38%. These results indicate that the space in the mesoporous silica internal pores was occupied by HRP molecules and clearly shows that the HRP molecules were mostly present inside the mesochannels of the MCM-41 materials, not on the outer surface of the crystals. The amounts of ovalbumin (OVA, $M_w \approx 43000$, molecular dimensions = 4.0 × 5.0 × 7.0 nm) and horseradish peroxidase (HRP, with similar molecular dimensions) adsorbed per unit weight of adsorbent are also listed in Table 1. On the parent MCM-41 material, similar adsorption levels were observed for OVA (119 mg/g) and HRP (125 mg/g). According to Takahashi et al., the maximum adsorption amount of HRP in conventional MCM-41 with a pore diameter of 5.0 nm is 98 mg/g,[15] ensuring that the parent MCM-41 material synthesized in this study had a quite large adsorption capacity. This might be due to the large pore volume derived from a well-defined geometry without secondary pores.

The P- and/or Ca-modified MCM-41 materials exhibited increased adsorption amounts of OVA and HRP and correspondingly showed larger occupancy rates compared with the parent MCM-41, regardless of their decreased pore volumes. The adsorbed amount of HRP increased in the following order: MCM-41 < Ca_{10}-MCM-41 < Ca_5P_5-MCM-41 < P_{10}-MCM-41. Furthermore, the occupancy rate more noticeably increased with increasing amount of TEP added to P/Si = 40 mol % (from 38% to 60% occupancy). In particular, P_{40}-MCM-41 afforded the highest uptake and occupancy rate of HRP, at 154 mg/g and 60%, respectively. From the molecular dimensions and the adsorbed amounts of HRP, we calculated that the volume of HRP adsorbed in the pores of MCM-41 was only 0.186 cm^3/g, which corresponds to 13.5% of the total free volume of MCM-41. On the other hand, the volume HRP molecules occupied in the pores of P_{40}-MCM-41 was calculated to be 0.230 cm^3/g, which corresponds to 22.5% of the total free volume of P_{40}-MCM-41. As the XRD results confirmed that the structures of the support materials remained unchanged after HRP immobilization, the large difference between the occupancy rate estimated from N_2 adsorption and that calculated from the adsorbed amounts can be attributed to the occlusion of mesochannels by large HRP molecules, which hinders nitrogen adsorption in the vacant spaces of the HRP-filled pores.[38]

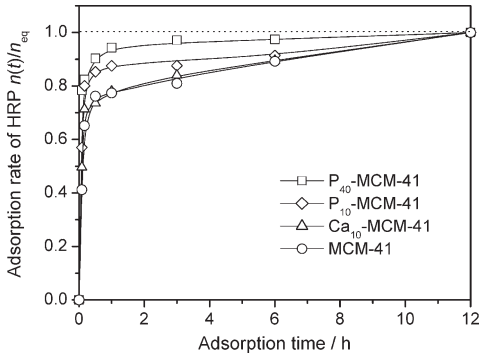

Figure 4. Adsorption time profiles of HRP molecules on MCM-41, P-modified MCM-41, and Ca-modified MCM-41 materials. Adsorption conditions: pH 7.0, buffer concentration = 50 mM, T = 4 °C.

From the experimental N_2 adsorption results, we conclude that HRP molecules are more closely packed inside the mesochannels of P- and/or Ca-modified MCM-41 materials than in those of unmodified siliceous MCM-41. This is presumably a consequence of the specific surface characteristics created by the P and/or Ca modification.

Time and pH Dependence of Enzyme Adsorption. The advantages of P and/or Ca atoms in enzyme adsorption can be determined by comparing their adsorption behaviors. Figure 4 shows the rate of HRP adsorption on P- and/or Ca-modified MCM-41 materials, expressed as $n(t)/n_{eq}$ (n_{eq} is the amount of HRP adsorbed at thermodynamic equilibrium after 12 h of adsorption) versus adsorption time t. The buffer concentration (50 mM), and adsorption temperature (4 °C) were kept constant in these experiments.

With increasing adsorption time, the adsorbed amount of HRP molecules increased, and the HRP adsorption finally reached adsorption equilibrium. Among the MCM-41 materials that we examined in this study, P-modified MCM-41 showed a higher rate of adsorption of HRP than the parent MCM-41 material, whereas Ca modification had little effect on the adsorption rate. The loading levels within the first 1 h of adsorption reached 88% and 94% for P_{10}-MCM-41 and P_{40}-MCM-41, respectively, whereas loading levels of only 77−78% were achieved for the parent MCM-41 and Ca_{10}-MCM-41 materials, clearly indicating that the P atoms facilitate the access of free HRP molecules to vacant adsorption sites in the internal pores.

In addition to the textural parameters of adsorbents, the solution pH is another important factor for determining adsorption amounts of enzymes, because pH alters the ionization degree of the functional groups of the enzyme and the surface charge of the adsorbents.[39] The pH profiles of the amounts of HRP adsorbed on the MCM-41 materials are shown in Figure 5. The adsorption capacities of HRP were found to vary markedly with the solution pH according to a bell curve, consistent with the report of Essa et al.:[39] All of the investigated mesoporous silica

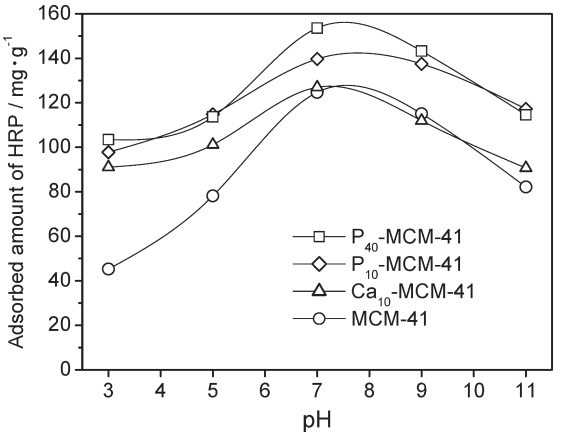

Figure 5. pH dependences of HRP adsorption on MCM-41, P-modified MCM-41, and Ca-modified MCM-41 materials. Adsorption conditions: adsorption time = 12 h, buffer concentration = 50 mM, T = 4 °C.

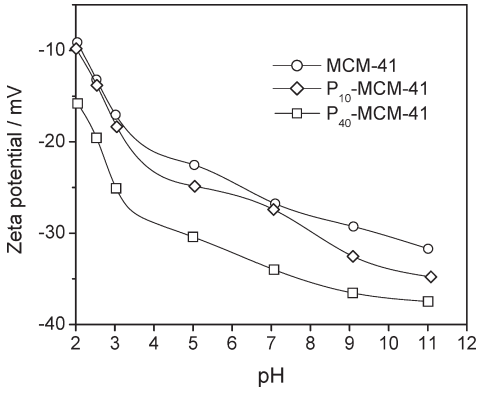

Figure 6. pH dependences of zeta potentials for MCM-41 and P-modified MCM-41 materials.

supports showed the highest adsorbed amounts at pH 7.0, and the adsorbed amounts decreased significantly above and below pH 7.0. Such a pH dependence can be strongly associated with electrostatic interactions between enzymes and the solid surfaces of adsorbents.

To gain insight into the surface charge of the MCM-41 supports, zeta potentials were measured. Figure 6 displays the pH dependences of the zeta potential for MCM-41 and P-modified MCM-41. As expected, the MCM-41 materials prepared in this work were all negatively charged in the pH range of 3−11, and it was found that the more negatively charged surfaces were created by P modification. The isoelectric point (pI) of the HRP molecule is known to be between pH 6 and 7.[29] This pI value of proteins fundamentally depends on the balance of surface functional groups (e.g., $-NH_2$, −COOH) and plays a crucial role in the adsorption behavior according to the solution pH.

The maximum adsorbed amount of 125 mg/g for the parent MCM-41 material was observed near the isoelectric point, at pH 7.0. At this pH, the net charge of the HRP molecule is minimized; consequently, the Coulombic repulsive force between HRP molecules would be minimal, and thus, closer packing of the protein molecules inside the mesochannels would be allowed. Under such conditions, hydrogen bonding between the amide groups of HRP and the silanol groups on the MCM-41 surface or

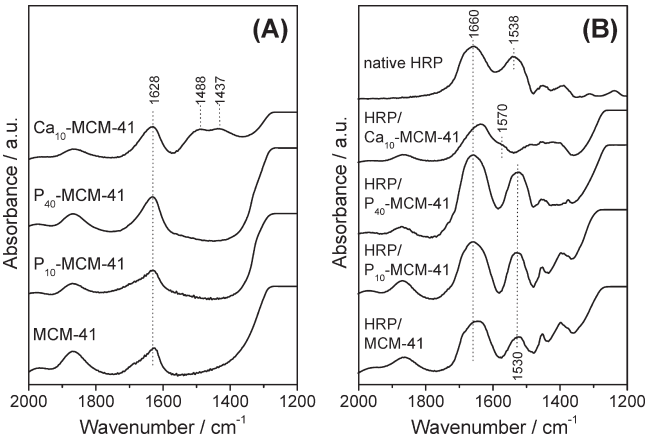

Figure 7. Infrared spectra of MCM-41 materials (A) before and (B) after HRP immobilization.

hydrophobic interactions between the alkyl groups of HRP and the siloxane bridges of MCM-41 are predominant. The decreased HRP adsorption at lower pH (pH 3−5) can be attributed to the increased positive charge on the HRP molecules, which induces enzyme−enzyme repulsion and restricts close packing of the HRP molecules, thus leading to a low adsorption capacity. Another plausible reason for this decrease is the reduced negative charge density of the MCM-41 surface; that is, the electric charge gradually approaches neutral at lower pH and reduces the enzyme−surface electronic interaction. On the other hand, when the solution pH is above the isoelectric point (pH 9−11), the overall negative charges of the HRP molecules and MCM-41 surface increase. This causes electrostatic enzyme−enzyme and enzyme−surface repulsion and hinders the adsorption of HRP on the silica surface, resulting in a low adsorption capacity.

Notably, P-modified MCM-41 materials exhibited improved adsorption properties at all pH values, particularly at very low pH (pH = 3−5), compared to the parent MCM-41 material. This is a consequence of the strongly negatively charged surface of P-modified MCM-41 materials, confirmed by zeta potential measurements: When the adsorption is performed at a pH lower than the isoelectric point where the protein molecules are positively charged, a stronger electrostatic attractive force occurs for the more negatively charged surface of P-modified MCM-41.

FT-IR spectroscopy can provide additional useful information about the interaction between the adsorbed HRP molecules and the surface of the adsorbents, as well as the molecular conformation of HRP. As shown in Figure 7B, native HRP exhibits several sharp absorption bands at 1538 and 1660 cm^{-1}. The former is assigned to the bending and stretching modes of the N−H and C−N bonding of amide groups (amide II), and the latter is attributed to C═O stretching of the α-helical conformation of HRP molecules (amide I).[14,40] The peak intensities and positions of these amide bands are typically used for the determination of the conformation and unfolding of the proteins. In the infrared spectra of HRP-immobilized MCM-41, P_{10}-MCM-41, and P_{40}-MCM-41, distinct shifts of the amide II bands (from 1538 to 1530 cm^{-1}) were observed, indicating the preservation of the integrity of the protein structure even after HRP immobilization and the strong chemisorption between the amide groups of HRP and the hydrated silica surface. Considering the zeta potential and FT-IR results, it is likely that the P atoms attached on the silica surface work as additional anionic sites available for enzyme

Scheme 1. Schematic Illustration of the Adsorption Kinetics of HRP Molecules on P- or Ca-Modified MCM-41

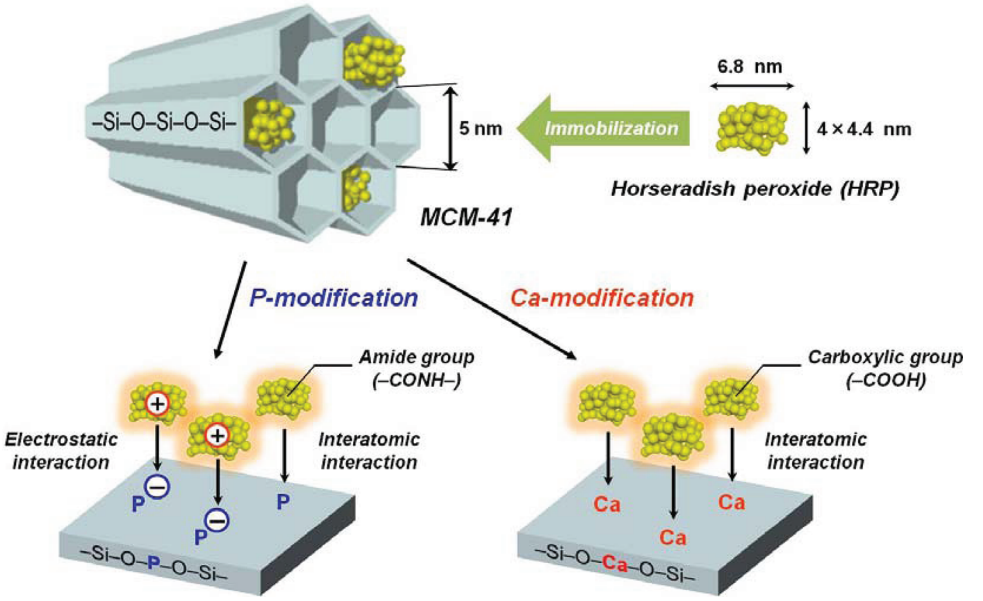

adsorption and also provoke local interactions with the cationic amide groups of HRP molecules (Scheme 1), which might allow the rapid adsorption and improved adsorption capacity in the high pH range demonstrated in Figures 4 and 5, respectively. The suggested adsorption kinetics is closely similar to that on −COOH-functionalized mesoporous silicas, that is, electrostatic interaction between positively charged enzyme molecules and a negatively charged solid surface.

On the other hand, Ca_{10}-MCM-41 also showed an improved adsorption capacity at pH values below pH 7.0, although not to the same extent as P_{10}-MCM-41. This result cannot be explained solely in terms of the strength of the surface charge. As mentioned previously, the infrared spectra of the Ca_{10}-MCM-41 samples (Figure 7A) exhibited some characteristic absorption bands assignable to siloxane bonding (1200−1350 cm^{-1}) and O−H bending of silanol groups (1628 cm^{-1}), as well as some broad absorption bands at around 1437 and 1488 cm^{-1} that can be assigned to carbonate species (CO_3^{2-}) physisorbed from the air. After the immobilization of HRP on the Ca_{10}-MCM-41 materials, no characteristic absorption band attributable to functional groups of HRP molecules, except for a shoulder peak at around 1570 cm^{-1}, was observed (Figure 7B), implying the denaturation of the protein structure of the HRP molecules. The increased adsorption capacity on Ca_{10}-MCM-41 is therefore conceivably due to chelation between the anionic carboxylic groups of thus-cleaved protein molecules and cationic Ca atoms, which might appear as a peak at 1570 cm^{-1} in the FT-IR spectrum.

A prominent adsorption capacity of P-modified MCM-41 was observed in the adsorption of OVA (pI = 4.9) as well,[7] where the maximum adsorption capacity was again observed at around the isoelectric point of OVA (pH 5), as can be deduced from the HRP adsorption results. Thus, it has been practically demonstrated that the surface charge of the adsorbents and the specific interaction between adsorbents and biomolecules significantly influence the uptake of the biomolecules. Most importantly, anionic P atoms and cationic Ca atoms on the silica surface are responsible for the rapid and large uptake of proteins, although they contribute in different manners. Additionally, FT-IR spectroscopy has revealed that the HRP molecules retain their correct protein structure on P-modified MCM-41 but lose it on Ca-modified MCM-41.

Enzymatic Activity in Organic Solvent. Because of its peroxidase activity, HRP has been widely utilized as a biocatalyst in applications for the decomposition of organic pollutants (e.g., dioxins, phenols, organophosphorus pesticides, and azo dyes), thereby diminishing the toxicity of industrial wastewaters.[41] However, the use of supported-enzyme catalysts still encounters some technological problems, such as the leaching of enzymes and conformational changes in proteins under specific reaction conditions, that frequently result in a crucial loss of enzymatic activity. For instance, solvent has a significant effect on these problems. Although the solubilization of enzymes in organic media could be advantageous in chemical reactions involving organic substrates, HRP-catalyzed reactions are usually conducted in a mixture of a hydrophilic organic solvent and an aqueous buffer solution, and an increase in the content of organic solvent often causes inactivation and leaching of enzymes.[42] Therefore, high stability against organic solvents is desirable for achieving homogeneity in the reaction and increasing the recyclability of biocatalysts.

To evaluate the effects of P and/or Ca modification on the enzymatic activity and structural stability of HRP, we examined the enzymatic activities of HRP-loaded MCM-41 catalysts under harsh conditions, using the oxidation reaction of 1,2-diaminobenzene with toluene and *tert*-butyl hydroperoxide (TBHP) as the organic solvent and oxidant, respectively, as a model reaction because of the high dispersibility of MCM-41 mesoporous silica in toluene.[15] The conversion rate was quantified by means of UV−vis spectroscopy.[35]

Figure 8 shows the time course of conversion in the 1,2-diaminobenzene oxidation reaction catalyzed by HRP immobilized on various MCM-41 materials and native HRP. The enzyme content for each reaction run was fixed at 1.0 mg to compare the net enzymatic activities. When HRP immobilized on the various MCM-41 supports was used, the amount of 1,2-diaminobenzene

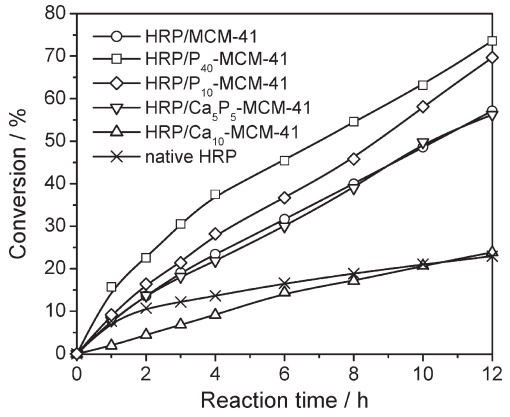

Figure 8. Conversions in the 1,2-diaminobenzene oxidation reaction catalyzed by HRP-immobilized MCM-41 materials and native HRP. Reaction conditions: enzyme, 1.0 mg each; substrate, 1 mmol in toluene; oxidant, 2.75 mmol in decane; pH 7.0; T = 37 °C.

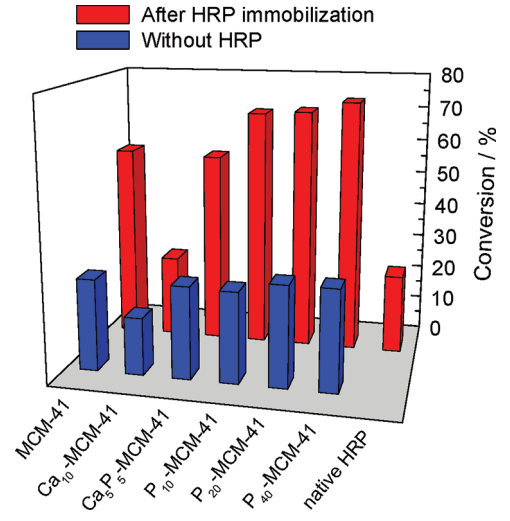

Figure 9. Comparison of catalytic activity of HRP-immobilized MCM-41 materials before (blue) and after (red) immobilization of HRP. Reaction conditions: enzyme, 1.0 mg each; substrate, 1 mmol in toluene; oxidant, 2.75 mmol in decane; pH 7.0; T = 37 °C; 12 h.

converted increased monotonically with increasing reaction time, and the corresponding polymeric compounds were obtained. On the contrary, direct addition of HRP resulted in an apparent loss of enzymatic activity after a couple of hours of reaction because of the denaturation of the protein structure. The oxidative activities of the corresponding weights of MCM-41 materials were also tested to measure the background value. Figure 9 presents a comparison of the conversion rates of 1,2-diaminobenzene in 12 h before and after the HRP immobilization, demonstrating that the MCM-41 supports also function as oxidative catalysts that can mediate between the organic substrate and TBHP (26−29% conversion in 12 h, except for Ca_{10}-MCM-41, whose conversion was 16.7% in 12 h), although conversion was negligible without a catalyst. This is due to the inherent acidic nature of silica surfaces. As displayed in Figure 9, it was found that Ca modification reduced the oxidative activity of silica, whereas P modification of MCM-41 had little effect on the background value. This is possibly due to the high basicity of

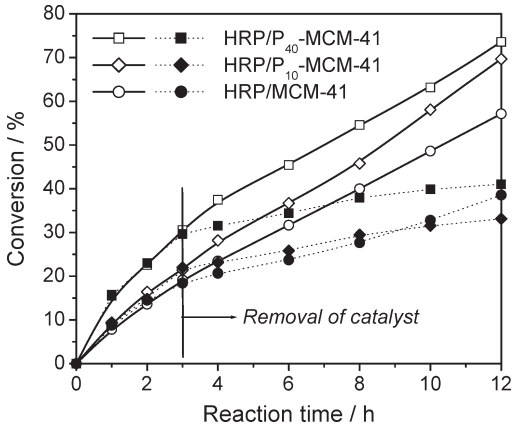

Figure 10. Effect of leaching of enzyme in the 1,2-diaminobenzene oxidation reaction without (solid lines) and with (dotted line) recovery of the solid catalysts from the reaction media after 3 h. Reaction conditions: enzyme, 1.0 mg each; substrate, 1 mmol in toluene; oxidant, 2.75 mmol in decane; pH 7.0; T = 37 °C.

Ca atoms, which might consume either TBHP or the catalytically generated radical species and inhibit the subsequent polymerization reaction.

HRP immobilized on the MCM-41 materials commonly exhibited relatively high enzymatic activities compared to the background data, demonstrating an enzyme-catalyzed nature of the polymerization reaction. The HRP immobilized on the MCM-41 material whose pore size matched the molecular size of HRP afforded 57.1% conversion in 12 h. This value is higher than the sum of the conversions of the native HRP (22.9%) and the parent MCM-41 support (26.9%), suggesting that the enzyme properly encapsulated in restricted pore spaces has an increased molecular recognition ability and is more resistant to organic solvents. Remarkably, the HRP immobilized on P-modified MCM-41 provided relatively high activity, and the enzymatic activity increased in the following order: P_{10}-CMM-41 (69.7%) < P_{20}-MCM-41 (70.5%) < P_{40}-MCM-41 (73.6%). This order is consistent with the order of the spatial occupancy and adsorption rates, as well as the strength of the surface negative charge. Meanwhile, HRP immobilized on Ca_5P_5-MCM-41, whose surface is made up of both cationic Ca and anionic P atoms, showed medium activity, 56.2% after 12 h, and HRP immobilized on Ca_{10}-MCM-41 exhibited a conversion rate (23.9%) similar to the background value (16.7%). Such poor activities are probably due to the basicity of Ca atoms as described above; otherwise, they might be due to the denaturation of the protein structure as confirmed by FT-IR spectroscopy. These experimental results clearly indicate that a support having a basic surface is not suited for enzymatic oxidation reactions, although mesoporous silica bearing Ca atoms can provide a surface environment suited for protein adsorption.

To examine the possibility that the reaction is homogeneously catalyzed by HRP leached into the reaction solution, three samples, namely, HRP immobilized on each unmodified MCM-41, P_{10}-MCM-41, and P_{40}-MCM-41, were chosen and tested in the same reaction with recovery of the solid catalysts from the reaction medium after 3 h. Figure 10 compares the conversion rates in the 1,2-diaminobenzene oxidation reaction with and without recovery of the solid catalysts. After the removal of the solid catalysts, the conversion rates decreased markedly, but the reactions were never quenched. Any further reaction after

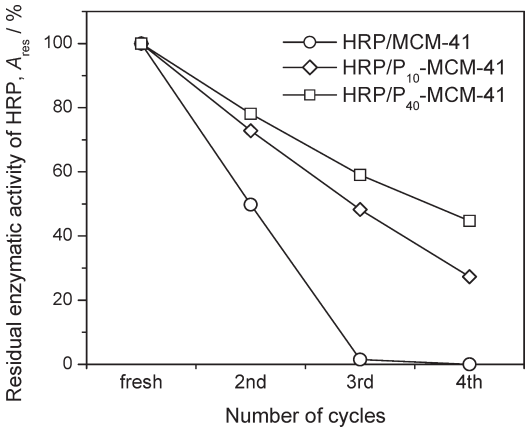

Figure 11. Influence of repetitive cycles on enzyme leaching for HRP immobilized on MCM-41 and P-modified MCM-41.

3 h must be due to catalysis by free HRP left in the reaction medium, indicating significant leaching of the enzymes from the MCM-41 supports under such harsh reaction conditions. Nevertheless, when P-MCM-41 materials were used as supports, only ca. 11% of the organic substrate was catalyzed by free HRP after the removal of the solid catalysts, whereas use of the parent MCM-41 material gave ca. 20% additional conversion. This encouraging result indicates that the degree of enzyme leaching is suppressed by P modification.

To assess the degree of leaching of enzyme from the mesoporous silica supports, these three samples were reused at least three times in the same reaction, where the solid catalysts were separated by centrifugation after 12 h of reaction, washed with 10 mL of toluene, stored at 4 °C until use, and then resuspended in the reaction solution to initiate the next catalytic run. The residual enzymatic activities (A_{res}) were determined by subtracting the background value to compare the net enzymatic activities. Figure 11 shows the leaching behaviors of HRP immobilized on MCM-41 and P-modified MCM-41 materials. Reused HRP supported on the parent MCM-41 material showed 50% of the activity of the fresh catalyst, and the residual activity reduced linearly upon the repeated use of the catalyst, demonstrating that purely siliceous MCM-41 allowed for considerable leaching during the reaction. This is due to the weak interaction between the enzyme molecules and the silica surface of MCM-41. In contrast, 73−78% of the initial activity was retained in the second catalytic run for immobilization on the P-MCM-41 materials, clearly demonstrating the benefit of P modification in suppressing the extent of enzyme leaching. Further reusability tests revealed that HRP immobilized on P-MCM-41 was enzymatically still active even after three continuous cycles under such harsh reaction conditions. In the fourth catalytic run, the residual enzymatic activities of HRP immobilized on P_{10}-MCM-41 and P_{40}-MCM-41 were 27.3% and 44.7%, respectively, of the initial activities, whereas HRP immobilized on MCM-41 lost all of its activity. It is believed that the strong interaction between the HRP molecules and the surface of P-modified MCM-41 prevented the unfolding and leaching of the enzyme, which resulted in a high enzymatic activity and recyclability.

CONCLUSIONS

We have successfully prepared P- and/or Ca-modified MCM-41 materials with suitable pore diameters and large pore volumes and found that the P and Ca atoms attached on the silica surface provide increased uptake of biomolecules. Detailed characterization by means of XRD, N_2 adsorption, FT-IR spectroscopy, and zeta potential measurements and enzyme adsorption experiments confirmed that the improved adsorption properties of P- and/or Ca-modified MCM-41 cannot be attributed solely to the quality of mesoporous structure, but should also be ascribed to the strong negative charge of the surface or the specific interatomic interaction between these atoms and the enzyme functional groups. In particular, P-modified MCM-41 showed improved adsorption capacity in a short adsorption period and over a wide pH range. Furthermore, P-modified MCM-41 was found to be effective for achieving stable storage of an enzyme and for protecting the enzyme from denaturation of its protein structure and leaching into an organic solvent, whereas Ca-modified MCM-41 inhibited activity for oxidation of the enzyme because of its basic character.

Because of the variety and complexity of biomolecules, it is important to create suitable chemical environments within the mesoporous silica nanospace depending on the nature of the biomolecules. Further advances in the above applications might require the extensive exploration of other heteroatoms and other types of enzymes. We believe that these materials could also be used for adsorption and separation of large toxic biomolecules and advantageously act as supports for the enzymatic conversion of bulky organic molecules.

ASSOCIATED CONTENT

Supporting Information. TEM images of mesoporous silica supports. This material is available free of charge via the Internet at http://pubs.acs.org.

AUTHOR INFORMATION

Corresponding Author
*E-mail: yamashita@mat.eng.osaka-u.ac.jp.

ACKNOWLEDGMENT

The present work was supported by Grants-in-Aid for Scientific Research (KAKENHI) from the Ministry of Education, Culture, Sports, Science and Technology (203603630 and 216562070). Y.K. acknowledges the JSPS Research Fellowships for Young Scientists. The authors appreciate Dr. Eiji Taguchi and Prof. Hirotaro Mori at the Research Center for Ultra-High Voltage Electron Microscopy, Osaka University, for assistance with TEM measurements.

REFERENCES

(1) (a) Willner, I.; Katz, E. *Angew. Chem., Int. Ed.* **2000**, *39*, 1181–1218. (b) Katz, E.; Willner, I. *Angew. Chem., Int. Ed.* **2004**, *43*, 6042–6108.

(2) Luckarift, H. R.; Spain, J. C.; Naik, R. R.; Stone, M. O. *Nat. Biotechnol.* **2004**, *22*, 211–213.

(3) (a) Gao, X.; Yu, K. M. K.; Tam, K. Y.; Tsang, S. C. *Chem. Commun.* **2003**, *9*, 2998–2999. (b) Huang, X.; Meng, X.; Tang, F.; Li, L.; Chen, D.; Liu, H.; Zhang, Y.; Ren, J. *Nanotechnology* **2008**, *19*, 445101. (c) Zhang, L.; Qiao, S.; Jin, Y.; Yang, H.; Budihartono, S.; Stahr, F.; Yan, Z.; Wang, X.; Hao, Z.; Lu, G. Q. *Adv. Funct. Mater.* **2008**, *18*, 3203–3212.

(4) (a) Reisner, E.; Powell, D. J.; Cavazza, C.; Fontecilla-Camps, J. C.; Armstrong, F. A. *J. Am. Chem. Soc.* **2009**, *131*, 18457–18466. (b) Woolerton, T. W.; Sheard, S.; Reisner, E.; Pierce, E.; Ragsdale, S. W.; Armstrong, F. A. *J. Am. Chem. Soc.* **2010**, *132*, 2132–2133.

(5) Jung, D.; Streb, C.; Hartmann, M. *Microporous Mesoporous Mater.* **2008**, *113*, 523–529.
(6) Yiu, H. H. P.; Wright, P. A. *J. Mater. Chem.* **2005**, *15*, 3690–3700.
(7) Hartmann, M. *Chem. Mater.* **2005**, *17*, 4577–4593.
(8) Ispas, C.; Sokolov, I.; Andreescu, S. *Anal. Bioanal. Chem.* **2009**, *393*, 543–554.
(9) Lei, C.; Shin, Y.; Liu, J.; Ackerman, E. J. *J. Am. Chem. Soc.* **2002**, *124*, 11242–11243.
(10) (a) Galarneau, A.; Mureseanu, M.; Atger, S.; Renard, G.; Fajula, F. *New J. Chem.* **2006**, *30*, 562–571. (b) Mureseanu, M.; Galarneau, A.; Renard, G.; Fajula, F. *Langmuir* **2005**, *21*, 4648–4655.
(11) Weber, E.; Sirim, D.; Schreiber, T.; Thomas, B.; Pleiss, J.; Hunger, M.; Gläser, R.; Urlacher, V. B. *J. Mol. Catal. B: Enzym.* **2010**, *64*, 29–37.
(12) Tortajada, M.; Ramón, D.; Beltrán, D.; Amorós, P. *J. Mater. Chem.* **2005**, *15*, 3859–3868.
(13) Urabe, Y.; Shiomi, T.; Itoh, T.; Kawai, A.; Tsunoda, T.; Mizukami, F.; Sakaguchi, K. *ChemBioChem* **2007**, *8*, 668–674.
(14) Vinu, A.; Gokulakrishnan, N.; Balasubramanian, V. V.; Alam, S.; Kapoor, M. P.; Ariga, K.; Mori, T. *Chem.—Eur. J.* **2008**, *14*, 11529–11538.
(15) (a) Takahashi, H.; Li, B.; Sasaki, T.; Miyazaki, C.; Kajino, T.; Inagaki, S. *Microporous Mesoporous Mater.* **2001**, *44*−*45*, 755–762. (b) Takahashi, H.; Li, B.; Sasaki, T.; Miyazaki, C.; Kajino, T.; Inagaki, S. *Chem. Mater.* **2000**, *12*, 3301–3305.
(16) Mohajerani, B.; Soleymani-Jamarani, M.; Nazari, K.; Mahmoudi, A.; Moosavi-Movahedi, A. A. *J. Mol. Catal. A: Chem.* **2008**, *296*, 28–35.
(17) Park, M.; Park, S. S.; Selvaraj, M.; Zhao, D.; Ha, C. S. *Microporous Mesoporous Mater.* **2009**, *124*, 76–83.
(18) Prakasham, R. S.; Likhar, P. R.; Rajyalaxmi, K.; Subba Rao, C.; Sreedhar, B. *J. Mol. Catal. B: Enzym.* **2008**, *55*, 43–48.
(19) Yiu, H. H. P.; Botting, C. H.; Botting, N. P.; Wright, P. A. *Phys. Chem. Chem. Phys.* **2001**, *3*, 2983–2985.
(20) Pandya, P. H.; Jasra, R. V.; Newalkar, B. L.; Bhatt, P. N. *Microporous Mesoporous Mater.* **2005**, *77*, 67–77.
(21) Yamashita, H.; Mori, K.; Shironita, S.; Horiuchi, Y. *Catal. Surv. Asia* **2008**, *12*, 88–100.
(22) Trong, On, D.; Desplantier-Giscard, D.; Danumah, C.; Kaliaguine, S. *Appl. Catal. A: Gen.* **2001**, *222*, 299–357.
(23) Corma, A. *Chem. Rev.* **1997**, *97*, 2373–2420.
(24) (a) Vinu, A.; Murugesan, V.; Hartmann, M. *J. Phys. Chem. B* **2004**, *108*, 7323–7330. (b) Vinu, A.; Murugesan, V.; Tangermann, O.; Hartmann, M. *Chem. Mater.* **2004**, *16*, 3056–3065.
(25) Hench, L. L. *J. Mater. Sci. Mater. Med.* **2006**, *17*, 967–978.
(26) Yan, X.; Yu, C.; Zhou, X.; Tang, J.; Zhao, D. *Angew. Chem., Int. Ed.* **2004**, *43*, 5980–5984.
(27) (a) Vallet-Regí, M.; Ruiz-González, L.; Izquierdo-Barba, I.; González-Calbet, J. M. *J. Mater. Chem.* **2006**, *16*, 26–31. (b) López-Noriega, A.; Arcos, D.; Izquierdo-Barba, I.; Sakamoto, Y.; Terasaki, O.; Vallet-Regí, M. *Chem. Mater.* **2006**, *18*, 3137–3144. (c) Izquierdo-Barba, I.; Arcos, D.; Sakamoto, Y.; Terasaki, O.; López-Noriega, A.; Vallet-Regí, M. *Chem. Mater.* **2008**, *20*, 3191–3198.
(28) Li, X.; Wang, X.; He, D.; Shi, J. *J. Mater. Chem.* **2008**, *18*, 4103–4109.
(29) (a) Lobel, K. D.; Hench, L. L. *J. Sol*−*Gel Sci. Technol.* **1996**, *7*, 69–76. (b) Lobel, K. D.; Hench, L. L. *J. Biomed. Mater. Res.* **1998**, *39*, 575–579.
(30) Nakajima, A.; Takakuwa, K.; Kameshima, Y.; Hagiwara, M.; Sato, S.; Yamamoto, Y.; Yoshida, N.; Watanabe, T.; Okada, K. *J. Photochem. Photobiol. A: Chem.* **2006**, *177*, 94–99.
(31) Lindlar, B.; Kogelbauer, A.; Kooyman, P. J.; Prins, R. *Microporous Mesoporous Mater.* **2001**, *44*−*45*, 89–94.
(32) Vallet-Regí, M.; Izquierdo-Barba, I.; Rámila, A.; Pérez-Pariente, J.; Babonneau, F.; González-Calbet, J. M. *Solid State Sci.* **2005**, *7*, 233–237.
(33) Xue, W.; Bandyopadhyay, A.; Bose, S. *Acta Biomater.* **2009**, *5*, 1686–1696.
(34) Li, X.; Shi, J.; Zhu, Y.; Shen, W.; Li, H.; Liang, J.; Gao, J. *J. Biomed. Mater. Res. B: Appl. Biomater.* **2007**, *83*, 431–439.
(35) Sayyah, S. M.; El-Deeb, M. M.; Kamal, S. M.; Azooz, R. E. *J. Appl. Polym. Sci.* **2009**, *112*, 3695–3706.
(36) Szu, S. P.; Klein, L. C.; Greenblatt, M. *J. Non-Cryst. Solids* **1992**, *143*, 21–30.
(37) Rehman, I.; Bonfield, W. *J. Mater. Sci. Mater. Med.* **1997**, *8*, 1–4.
(38) Miyahara, M.; Vinu, A.; Ariga, K. *Mater. Sci. Eng, C* **2007**, *27*, 232–236.
(39) Essa, H.; Magner, E.; Cooney, J.; Hodnett, B. K. *J. Mol. Catal. B: Enzym.* **2007**, *49*, 61–68.
(40) Adams, S.; Higgins, A. M.; Jones, R. A. L. *Langmuir* **2002**, *18*, 4854–4861.
(41) (a) Dordick, J. S.; Marletta, M. A.; Klibanov, A. M. *Biotechnol. Bioeng.* **1987**, *30*, 31–36. (b) Kamiya, N.; Okazaki, S.; Goto, M. *Biotechnol. Technol.* **1997**, *11*, 375–378.
(42) Zaks, A.; Russell, A. J. *J. Biotechnol.* **1988**, *8*, 259–269.